International Journal of Nanomedicine

Dovepress
open access to scientific and medical research

Open Access Full Text Article

ORIGINAL RESEARCH

Sesamol-Loaded PLGA Nanosuspension for Accelerating Wound Healing in Diabetic Foot Ulcer in Rats

This article was published in the following Dove Press journal:
International Journal of Nanomedicine

Karthik Gourishetti[1]
Raghuvir Keni[1]
Pawan Ganesh Nayak[1]
Srinivas Reddy Jitta[2]
Navya Ajitkumar Bhaskaran[2]
Lalit Kumar[2]
Nitesh Kumar[1]
Nandakumar Krishnadas[1]
Rekha Raghuveer Shenoy[1]

[1]Department of Pharmacology, Manipal College of Pharmaceutical Sciences, Manipal Academy of Higher Education, Manipal 576104, Karnataka, India; [2]Department of Pharmaceutics, Manipal College of Pharmaceutical Sciences, Manipal Academy of Higher Education, Manipal 576104, Karnataka, India

Background: Diabetic foot ulcer is an intractable complication of diabetes, characterized by the disturbed inflammatory and proliferative phases of wound healing. Sesamol, a phenolic compound, has been known for its powerful antioxidant, anti-inflammatory, anti-hyperglycaemic and wound healing properties. The aim of the present study was to develop a sesamol nano formulation and to study its effect on the various phases of the wound healing process in diabetic foot condition.

Methods: Sesamol-PLGA (SM-PLGA) nanosuspension was developed using nanoprecipitation method. TEM, in vitro drug release assay and in vivo pharmacokinetic studies were performed for the optimised formulation. Diabetic foot ulcer (DFU) in high fat diet (HFD)-fed streptozotocin-induced type-II diabetic animal model was used to assess the SM-PLGA nanosuspension efficacy. SM-PLGA nanosuspension was administered by oral route. TNF-α levels were estimated using ELISA and Western blot analysis was performed to assess the effect on the expression of HSP-27, ERK, PDGF-B and VEGF in wound tissue. Wound re-epithelization, fibroblast migration, collagen deposition and inflammatory cell infiltration were assessed by H&E and Masson's trichrome staining. Effect on angiogenesis was assessed by CD-31 IHC staining in wound sections.

Results: The optimized SM-PLGA nanosuspension had an average particle size of <300 nm, PDI<0.200 with spherical shaped particles. Approximately 80% of the drug was released over a period of 60 h in in vitro assay. Half-life of the formulation was found to be 13.947 ± 0.596 h. SM-PLGA nanosuspension treatment decreased TNF-α levels in wound tissue and accelerated the collagen deposition. Whereas, HSP-27, ERK, PDGF-B and VEGF expression increased and improved new blood vessels' development. Rapid re-epithelization, fibroblast migration, collagen deposition and reduced inflammatory cell infiltration at the wound site were also observed.

Conclusion: Results indicate that sesamol-PLGA nanosuspension significantly promotes the acceleration of wound healing in diabetic foot ulcers by restoring the altered wound healing process in diabetic condition.

Keywords: diabetes, diabetic foot ulcer, sesamol, PLGA, nanosuspension, controlled release, wound healing, re-epithelization, angiogenesis, TNF-α

Correspondence: Rekha Raghuveer Shenoy
Department of Pharmacology, Manipal College of Pharmaceutical Sciences, Manipal Academy of Higher Education, Manipal 576104, Karnataka, India
Tel +91-820-2922482
Fax +91-820-2571998
Email rekhaarunt@gmail.com

Introduction

Diabetes mellitus, a metabolic disorder characterized by unusual glucose metabolism, mainly occurs due to the loss of sensitivity of insulin and its receptors. A person with diabetes is 25% likely to suffer from diabetic foot ulcer (DFU). In addition, the probability of lower leg amputation due to diabetic complications rises to 84% during the individual's lifetime.[1] Diabetic foot ulcer (DFU) is characterized by the disturbed

submit your manuscript | www.dovepress.com
DovePress
http://doi.org/10.2147/IJN.S268941

inflammatory and proliferative phases of wound healing. Elevated blood glucose levels decrease the wound healing process by increasing pro-inflammatory cytokines and proteases-1 which reduce growth factor levels, blood flow and cell migration. Impaired angiogenesis, cell proliferation and re-epithelization are hallmarks of diabetic wounds. The healing process can be improved by enhancing blood flow, cell proliferation, migration and angiogenesis which will further enhance the glucose uptake in muscle to reduce the blood glucose level.[2]

Sesamol (SM) [3, 4-methylenedioxyphenol] is a natural organic compound obtained from sesame oil.[3] It possesses hypolipidemic action, prevents oxidative stress[4] and is also found to have anti-clastogenic activity.[4,5] In our previous study, sesamol showed accelerated wound healing activity in dexamethasone-induced delayed wound healing model[6] by increasing the reepithelization and extracellular matrix (ECM) deposition. However, there are a few limitations with the pharmacokinetic properties of sesamol which limits its pharmacodynamic potential. Oral bioavailability of sesamol is around 35%[7] and the elimination of conjugated metabolites of sesamol is rapid (0–4 h).[8] Sesamol has good solubility in aqueous medium (38.8 mg/mL), with a pKa of 9.79 and a good lipophilicity of log P 1.29. SM is well absorbed throughout the gastrointestinal tract (85% through stomach). In order to improve the therapeutic potential of sesamol, it needs to be formulated in a suitable delivery system, which controls its release profile, prolongs circulation in the body and prevents rapid elimination from the systemic circulation.[9]

Diabetic foot ulcer management is one of the areas where researchers are showing keen interest on developing various kinds of formulations and wound dressings using nanotechnology. An extensive review was given by Mei Shao et al[10] and Zahid Hussain et al about recent developments in drug delivery systems and polymer-based wound dressings for the diabetic foot ulcer management.[11]

One solution to this issue of bioavailability is to use poly (lactic-co-glycolic acid) or PLGA based conjugates encapsulated to form nanoparticles. Nanotechnology is a new area of research where the use of topical formulations can help achieve improvement in the aqueous solubility and bioavailability.[12] These nano-delivery systems allow continuous and long-term administration of hydrophilic and lipophilic drugs to the target sites. PLGA would allow for a higher drug carrying capacity than other polymers, it has better stability and allows for a lower dosing frequency and can be administered in a variety of ways. Hence, we prepared sesamol loaded PLGA (SM-PLGA) nanosuspension to improve the pharmacokinetic profile of sesamol which will reduce the microvascular complications of diabetes. We evaluated the effect of the prepared nano-formulation at different phases of healing in diabetic foot ulcer in high fat diet (HFD) and low dose streptozotocin-induced diabetic rats.

Materials and Methods

Sesamol, dialysis membrane and polyvinyl alcohol (PVA molecular 30000–70000) were obtained from Sigma-Aldrich Co. LLC (St. Louis, MO, USA). PLGA (50:50) [(Resomer® RG 502 H, Poly (D, L-lactide-co-glycolide)] was a gift sample from Evonik India Pvt. Ltd. (Mumbai, India). Streptozotocin (STZ) was procured from MP Biomedicals India Pvt. Ltd. (Navi Mumbai, India). Glucose strips were procured from Alere Medical Pvt. Ltd. (Gurugram, India).

FloroTrans® PVDF membrane obtained from Pall Corporation (Port Washington, NY, USA). Western blot buffers procured from Bio-Rad Laboratories (India) Pvt. Ltd. (Gurugram, India). VEGF-A, PDGF -B, CD-31 antibodies procured from Abcam PLC (Cambridge, UK). HSP-27 and Phospho HSP-27, ERK and P-ERK primary antibodies procured from Elabscience Inc. (Wuhan, Hubei, China). GAPDH obtained from Sigma-Aldrich Co. LLC (St. Louis, MO, USA). IHC development kit obtained from Enzo Life Sciences Inc. (Farmingdale, NY, USA). TNF-alpha ELISA kit and BCA Protein Assay kit were procured from Thermo Fischer Scientific India Pvt. Ltd. (Mumbai, India). Secondary antibody (HRP labelled) obtained from The Jackson Laboratory (Bar Harbor, ME, USA). West Bright ECL chemiluminescent HRP substrate obtained from Advansta Inc. (San Jose, CA, USA).

Preparation of Sesamol-PLGA (SM-PLGA) Nanosuspension

SM-PLGA nanoparticles were prepared by a previously described method[13] with a few modifications. Briefly, SM (100 mg) and PLGA (50:50) (200 mg) was dissolved in 3 mL of acetone (organic solution). PVA solution 20 mL (stabilizer) was taken in a 50 mL glass beaker and was kept on an ice bath. The drug dissolved in the organic solution and polymer was added dropwise into the PVA solution with continuous homogenization (Polytron PT-MR 3100; Kinematica AG, Luzern, Switzerland) for 5 min at 15000 RPM. After homogenization, the preparation was subjected to sonication immediately (Ultrasonic

Processor, VC 130; Sonics & Materials Inc., Newton, CT, USA) at 80 amplitude for specified time using 10 s pulses. Finally, the prepared nano-formulation was subjected to magnetic stirring (3 h) at room temperature for the removal of organic solvent.

Solid State Characterization

Differential Scanning Calorimetry (DSC) and Fourier-transform Infrared (FTIR) analysis was used to determine the compatibility of drug and excipients.

Differential Scanning Calorimetry (DSC)

Approximately 5 mg of the sample was weighed and placed in the bottom half of the aluminium DSC pan and crimped. The same procedure was followed for an empty aluminium pan and was used as a reference sample. The prepared samples were heated up to 120 °C keeping the temperature ramp up at a rate of 10 °C per minute in an atmosphere of nitrogen. The thermograph of the drug (sesamol) and a physical mixture of drug with polymer (PLGA) were obtained with the help of DSC 60 Plus Calorimeter with TA-60 WS Thermal Analyser from Shimadzu Corporation (Kyoto, Japan).

Fourier-Transform Infrared (FTIR)

200 mg of potassium bromide (KBr) was transferred into an agate mortar and ground it to a fine powder until crystallites were no longer visible to the naked eye and the compound turned a little pasty and stuck to the mortar slightly. The pure drug powder 4 mg (about 2% total of KBr) was taken and mixed with the ground KBr powder to get a homogeneous mixture and to reduce the particle size to less than 5 mm in diameter. This was done since the large particles scatter the infrared beam and cause the sloping baseline of the spectrum. This mixture was further compressed into a disc by applying a compression force of 5 tons for 5 min in a hydraulic press. The flattened disc of the sample was in the path of light and the spectra was recorded. The spectra of the drug and binary mixture (drug and lipid in the ratio 1:1) were obtained at a wavelength of 400–4000 cm^{-1} with the help of FTIR spectrophotometer (FTIR-8300, Shimadzu Corporation, Kyoto, Japan) configured with IR solution v.1.2 software.

Physicochemical Characterization of Sesamol PLGA Nanosuspension

Particle Size and Zeta Potential

Zetasizer (ZEN 3600; Malvern Instruments Ltd., Malvern, UK) was used for the analysis of particle size, polydispersity index (PDI) and zeta potential. The SM-PLGA nanosuspension was diluted 10 times with Type-I water to produce the working concentration. Subsequently, the diluted suspension (1 mL) was transferred into zeta cell. Later, the cell was fixed into zetasizer to record the zeta potential. Similarly, diluted SM-PLGA nano-suspension was placed in a transparent glass cell to record the particle size and dialysis of samples were carried out at 90° scattering angle at 25 °C.[13,14]

Encapsulation Efficiency (EE)

The encapsulation efficiency of SM-PLGA nanosuspension was measured spectrophotometrically at 294 nm by estimating the free sesamol in supernatant (indirect method). Briefly, for presence of free drug in SM-PLGA formulation, 0.5 mL of the formulation and blank formulations were taken in two different microcentrifuge tubes and diluted with 0.5 mL of Type-I water which was centrifuged using cooling centrifuge (3K30, Sigma Laborzentrifugen GmbH, Germany) at 54,200 g for 30 min at 4 ºC. The supernatant was collected and filtered using a syringe filter (0.22 µ). The absorbance of filtrate was measured at 294 nm by using UV-Spectrophotometer (UV-1601PC, Shimadzu Corporation, Kyoto, Japan). The entrapment efficiency (EE) of SM-PLGA nanosuspensions was calculated using the formula:[15,16]

$$\text{Entrapment efficiency}(\%) = \left(\frac{\text{Initial drug amount} - \text{free drug after encapsulation}}{\text{Initial drug amount}}\right) \times 100$$

Transmission Electron Microscopy (TEM) Analysis

Shape and surface morphology of the optimized batch of SM-PLGA nanosuspension were observed using TEM (CM200, Philips Co., Amsterdam, The Netherlands) by staining the sample with a 2% w/v of phospho-tungstic solution (pH 6.0). A drop of the formulation (200 times diluted) was placed on a carbon-coated copper grid. Then, the film was negatively stained using the phospho-tungstic acid solution and the grid was dried. Thereafter, the sample was observed under TEM.

In vitro Drug Release Study

In vitro drug release of an optimized nanosuspension was carried out by taking the SM-PLGA (4 mL) in a dialysis membrane (molecular cut-off 12–14 kDa) while closing the ends with dialysis clips and suspending in the

dissolution medium (phosphate buffer pH 6.8). The study was carried out using United States Pharmacopeia (USP) type II dissolution apparatus. The same procedure was followed for the standard while taking the drug (5 mg/mL) in 4 mL Type-I water. Volume of dissolution used in the study was 500 mL. The speed of the paddle and temperature of the medium were maintained at 50 rpm and 37 °C ± 0.5 °C, respectively. The samples (2 mL) were collected at predetermined time intervals and sink conditions were maintained throughout the experiment by replacing the same volume of the sample with blank phosphate buffer. The collected samples were filtered, diluted and analysed by UV-Spectrophotometer.

In vivo Studies

Pharmacokinetic Studies

Pharmacokinetic study of the nanosuspension of sesamol and plain drug dispersion was performed on male Wistar rats (200–250 g). The animals were acclimatized at 24–26 °C and maintained in 12 h dark and 12 h light cycle and animals had free access to normal chow diet and water ad libitum. The animal experiment protocol was reviewed and approved by Institutional Animal Ethics Committee (IAEC), Kasturba Medical College, Manipal Academy of Higher Education, Manipal (IAEC/KMC/98/2017). All animal experiments were performed as per the Committee for the Purpose of Control and Supervision on Experiments on Animals (CPCSEA) guidelines.

Animals were randomly divided into standard and test groups (n=6 animals in each group). The standard group received standard drug (sesamol) dispersed in 0.25% (w/v) sodium CMC (sodium carboxy methyl cellulose) at the dose of 50 mg/kg body weight; similarly, test group received nanosuspension at the dose of 50 mg/kg body weight. Blood (500 µL) was withdrawn from retro-orbital at different time intervals from 0 h to 72 h from each rat in a microcentrifuge tube containing 20 µL of dipotassium EDTA. Plasma was separated by centrifuging the blood samples at 4 °C and 10000 RPM for 10 min. The separated plasma samples were stored at −80 °C until further analysis.

Drug analysis in the plasma was determined using HPLC briefly, a simple isocratic, sensitive, fast HPLC bioanalytical method was developed for the quantification of sesamol in rat plasma. Sesamol was extracted from rat plasma using protein precipitation method and methanol was used as the precipitation solvent. Hyper Clone BDS C_{18} column of 250 mm length with 4.6 mm internal diameter and 5 µm particle size with a pore size of 130 Å was used for the separation. The column was maintained at a temperature of 25 °C in column oven compartment. Acetonitrile and 0.1% formic acid in Type-I water was used as the mobile phase. The mobile phase was pumped at a flow rate of 0.6 mL/min in an isocratic mode in the ratio of 50:50% v/v (acetonitrile: 0.1% formic acid in Type-I water) for a total run time of 8 min. The eluent from the column was monitored at a wavelength of 298 nm using UV detector. The plasma drug concentrations obtained were used for the calculation of pharmacokinetic parameters such as C_{max}, T_{max}, AUC, half-life ($t_{1/2}$), mean residence time (MRT), apparent volume of distribution (V_d) and elimination rate constant (K_e) by - WinNonlin® software using non-compartmental method (NCA).

In vivo Wound Healing Study in Diabetic Foot Ulcer Animal Model

Induction of Diabetes

Type-2 diabetes was induced by previously described methods with few modifications.[1,17] Briefly, rats were randomly divided in to two groups one is control group (n=18) and type 2 diabetic group (n=90), control group was fed with standard chow diet and diabetic group was fed with in-house prepared HFD (58% calories as fat)[17] for a period of 8 weeks. After 8 weeks of HFD feeding, the rats of type-2 diabetic group animals were kept on overnight fasting and low dose streptozotocin (35 mg/kg) injection was given by intraperitoneal route. The rats were allowed to develop diabetes for 4 weeks.[18] At 3, 6 or 8 weeks after feeding and 4 weeks after STZ injection, the body weight was recorded for all the rats.

Oral Glucose Tolerance Test (OGTT)

After HFD or normal diet intervention, rats were fasted overnight then given an oral administration of glucose with a dose of 2 g/kg body weight. Blood glucose (BG) levels were determined before and after 15, 30, 60, 90 and 120 min of the glucose administration.

Measurement of Fasting Blood Glucose Levels

After 4 weeks of STZ injection, animals were kept on fasting and blood glucose levels were measured with the help of Alere G1 glucometer. Those animals which were having fasting blood glucose levels above 350–400 mg/dL were selected for the study and randomized into 4 groups namely disease control, sesamol 50 mg/kg, sesamol 100 mg/kg, SM-

PLGA group (50 mg/kg) and normal control group (without diabetes) and fasting blood glucose levels were measured at day 0, day 7 and day 15.

Creation of Diabetic Foot Ulcer

After randomization, the animals were anesthetized with thiopental sodium (50 mg/kg) and a full thickness foot ulcer was made on dorsal hind foot by using Westcott scissor and 6 mm punch biopsy.[18]

Wound Healing Experiment

After creation of the foot ulcer animals were treated with respective treatments by oral route (normal control and disease control with saline, sesamol 50 mg/kg, sesamol

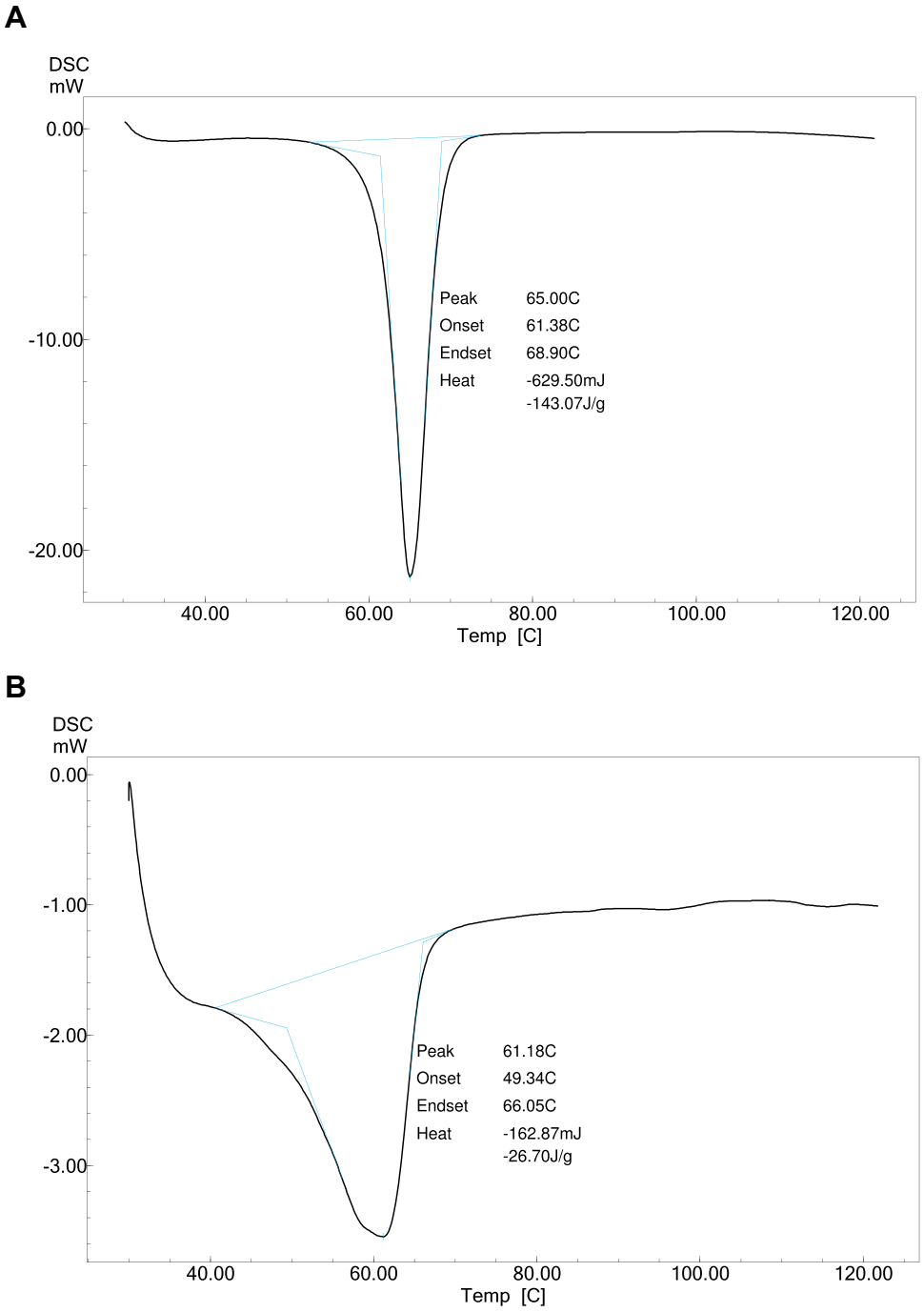

Figure 1 DSC thermogram of (**A**) Sesamol and (**B**) PLGA + PVA + Sesamol physical mixture.

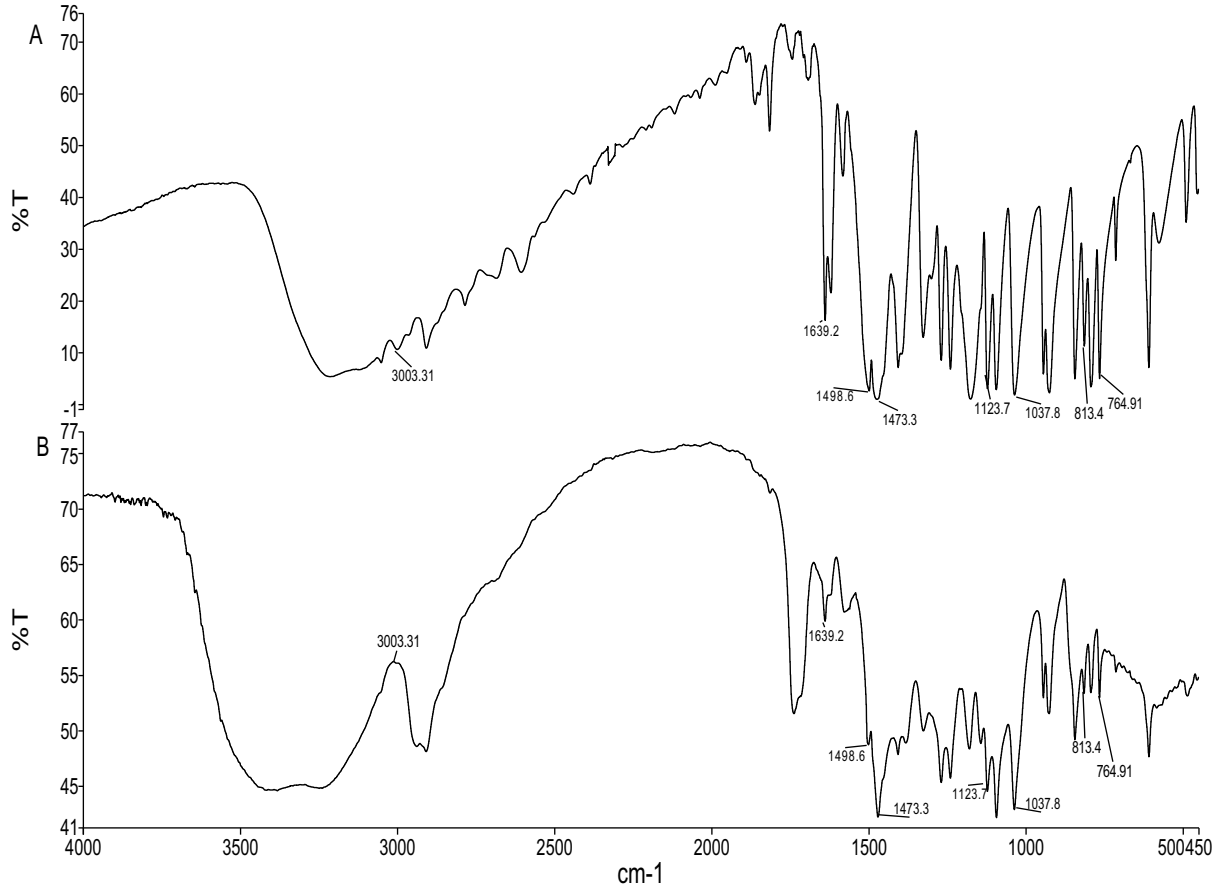

Figure 2 FTIR spectra of (**A**) Sesamol and (**B**) PLGA + PVA + Sesamol physical mixture.

100 mg/kg and sesamol-PLGA nanosuspension for a period of 15 days). 50 mg/kg and 100 mg/kg dose levels were selected based on previous studies.[19,20] After the treatment, the rats with diabetic foot ulcer were sacrificed (six animals for each group at each time point), foot ulcers were harvested and flash frozen with the help of liquid nitrogen for protein expression analysis. Samples collected for histopathological analysis, Masson trichome staining and immunohistochemical analysis, were fixed with formalin, dehydrated through a serial alcohol gradient, embedded in wax and 4 µM thickness longitudinal sections were used for further processing.

Table 1 Optimization and physicochemical characterization of SM-PLGA nanosuspension

S. No.	Polymer Weight	SM Amount (mg)	PVA (%)	Sonication Amplitude (W)	Sonication Time (Minutes)	Particle Size (nm)	PDI	ZP (-mV)	EE (%)
1	100	100	0.5	40	2.5	208.00±13.20	0.126±0.048	12.90±0.750	65.49±2.619
2	200	100	0.5	40	2.5	238.80±6.38	0.117±0.021	13.43±0.030	75.87±0.260
3	100	100	1	40	2.5	244.00±19.81	0.165±0.043	10.24±0.194	67.56±0.151
4	200	100	1	40	2.5	255.30±20.23	0.167±0.046	10.53±0.850	76.40±0.570
5	100	100	0.5	80	5	233.13±21.55	0.118±0.053	11.36±0.233	66.99±1.090
6	200	100	0.5	80	5	298.60±13.81	0.248±0.007	12.93±0.266	77.03±0.990
7	100	100	1	80	5	226.13±11.46	0.162±0.040	10.02±0.288	77.12±1.120
8	200	100	1	80	5	247.00±3.64	0.196±0.052	11.67±0.670	79.17±0.870

Note: Data represented as Mean ± SEM, n=3.
Abbreviations: SM, sesamol; PVA, polyvinyl alcohol; PDI, polydispersity index; ZP, zeta potential; EE, entrapment efficiency.

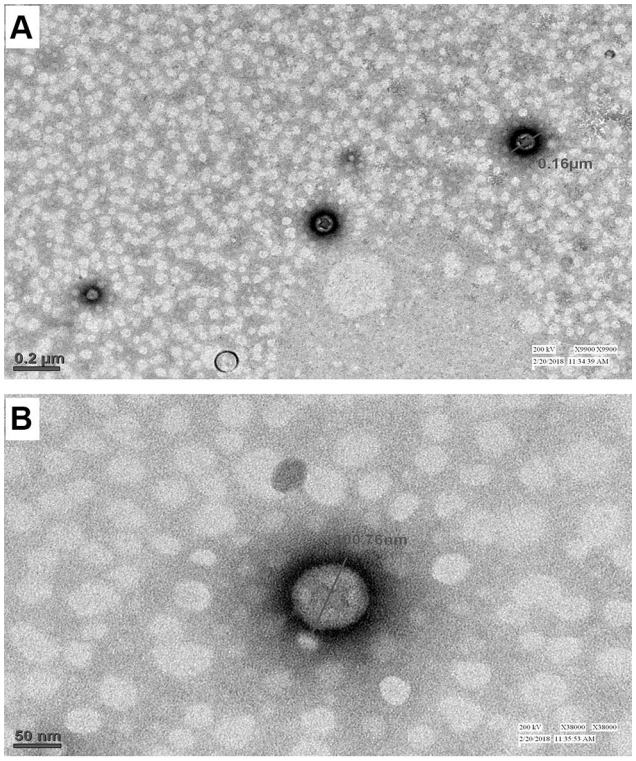

Figure 3 TEM images of optimized formulation at (**A**) 9900× resolution showing the particle size 160 nm, (**B**) 38000× resolution showing the internal architecture of the polymer matrix.

Measurement of Wound Closure

At every alternative day of the treatment, the wounds were photographed with a digital camera and then the wound size was analysed using ImageJ software. The percentage of wound closure was calculated by using the formula:

$$[\%\ of\ wound closure = \left(\frac{Initial\ day\ area - 5/10/15^{th}\ day\ area}{Initial\ day\ area}\right) \times 100$$

Western Blot

Wound tissues were homogenized with handheld tissue homogenizer in RIPA (Radio Immuno Precipitation Assay) lysis buffer (10%w/v) containing protease and phosphatase inhibitors in ice cold conditions and tissue lysates were centrifuged at 13000 RPM for 15 min. The supernatant was collected and stored at –80 °C until further analysis.

Total protein was analysed in tissue samples by using Pierce™ BCA Protein Assay kit. 30µg of protein from each sample was resolved and separated by 10% SDS-PAGE and transferred to a polyvinylidene difluoride membrane (PVDF). The membrane was blocked by 5% non-fat milk in Tris-buffered saline with Tween20 (TBST) and then incubated with VEGF-A, PDGF-B, HSP-27 and Phospho HSP-27, ERK and P-ERK, GAPDH primary antibody (all antibodies were used in 1:1000 dilution) in 5% BSA in TBST overnight at 4 °C. The membrane was then washed with TBST for 3 times, 10 min each to remove unbound primary antibody, then incubated with the secondary antibody tagged with HRP (1:10,000) for 90 min at room temperature and washed with TBST thrice. Bands were visualized with West Bright ECL chemiluminescent HRP substrate in Syngene G:Box Chemi XRQ gel documentation system. Relative quantities of protein were

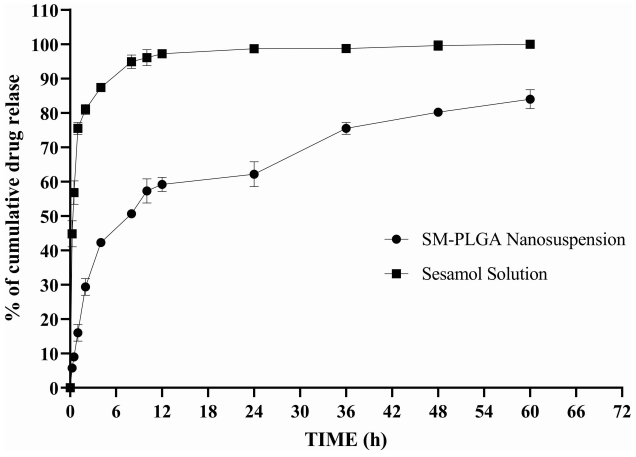

Figure 4 In vitro drug release profile of optimized SM-PLGA nanosuspension and sesamol solution at pH 6.8. Data represented as mean ± SEM, n=3.

Table 2 Pharmacokinetic parameters of standard and formulation group

Parameter	Standard Drug	SM-PLGA Nanosuspension
K_e (h^{-1})	0.367 ± 0.082	0.050 ± 0.002
$T_{1/2}$ (h)	2.097 ± 0.483	13.947 ± 0.596
T_{max} (h)	0.250 ± 0.500	60.000 ± 2.250
C_{max} (µg/mL)	65.056 ± 8.434	1153.780 ± 14.550
AUC_{0-t} (µg.h/mL)	24679.000 ± 3104.000	28649.298 ±1440.093
MRT (h)	0.849 ± 0.054	62.007 ± 0.347
V_d (L)	1.300 ±0.380	6.430 ± 0.132

Note: Data represented as mean ± SEM, n=3.

Abbreviations: C_{max}, peak plasma concentration; T_{max}, time to achieve peak plasma concentration; Ke, elimination rate constant; V_d, volume of distribution; AUC_{0-t}, area under the curve from the time of administration to time "t"; MRT, mean residence time.

determined using ImageJ densitometric analysis and presented in comparison with GAPDH expression.

TNF-α Estimation

In tissue lysates TNF-α was measured using rat TNF-α ELISA kit (Invitrogen, Thermo Fisher Scientific Inc., Waltham, MA, USA) and levels were expressed in pg/mg of protein.

Immuno-Histochemical and Histological Assessment of Wound Healing

For immunohistochemistry analysis, 4 µM thin sections were obtained from formalin-fixed paraffin-embedded tissues, and dewaxed in xylene and rehydrated through reducing concentration of ethanol and washed in phosphate buffer saline, antigen retrieval done with Tris-EDTA buffer (pH 9.0) and endogenous peroxidase activity was removed by incubating the sections in hydrogen peroxide solution (3%), then sections were blocked with 5% BSA for a period of 45 min then washed with phosphate buffer saline, then incubated with primary antibody CD-31 (1:200; Abcam PLC, Cambridge, UK) over night at 4 °C. Then sections were washed with phosphate buffer saline and incubated with HRP-labelled secondary antibody (Enzo Life Sciences Inc., Farmingdale, NY, USA) for 1 h at room temperature then sections were washed with phosphate buffered saline for three times and peroxidase activity was developed by incubating the sections with diaminobenzidine tetrahydrochloride (DAB) for 5 min at room temperature, then the sections were observed under microscope and the stained (brown colour) regions were counted with ImageJ software.

For epidermal regeneration, granulation tissue formation, inflammatory cell infiltration, neovascularization, and collagen deposition the sections were stained with haematoxylin and eosin and Masson's trichome staining.

Scoring of histological parameters were done from minimal to moderate to indicate the degree of healing in DFU conditions.[21] Histology scoring for epidermal regeneration, granulation tissue formation, inflammatory cell infiltration, neovascularization and collagen deposition was represented as +, ++, +++ (+ Mild, ++ Moderate, +++ Extensive).

Statistical Analysis

The results are expressed in mean ± SEM, statistical analysis was performed using GraphPad Prism version 8.4.3 for Windows (GraphPad Software LLC, La Jolla, CA, USA) by unpaired *t*-test, one-way ANOVA and two-way ANOVA with Tukey's post hoc and/or Bonferroni post hoc test for paired comparisons of means.

Results and Discussion

Solid State Characterization

Differential Scanning Calorimetry (DSC)

The DSC thermogram of pure sesamol (Figure 1A) showed a sharp endotherm maximum melting point at 65.00 °C. The DSC thermogram of a physical mixture of

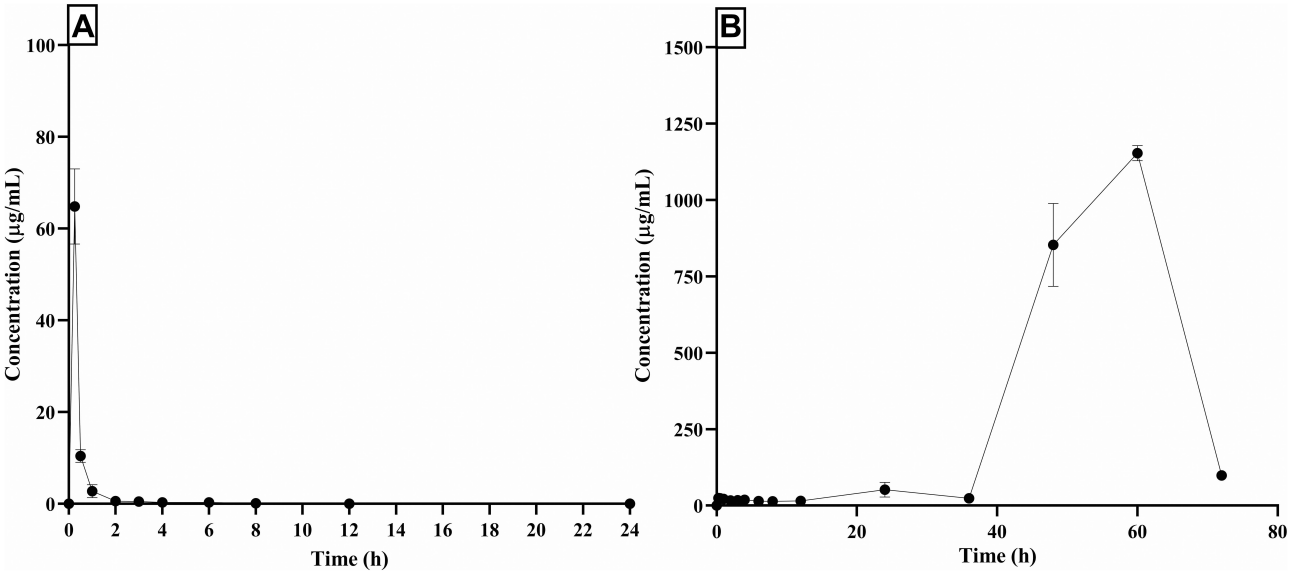

Figure 5 Plasma concentration vs time graph of standard drug and optimized SM-PLGA nanosuspension. Plasma drug release profile (**A**) Sesamol standard drug (**B**) SM-PLGA nanosuspension. Data represented as mean ± SEM, n=3.

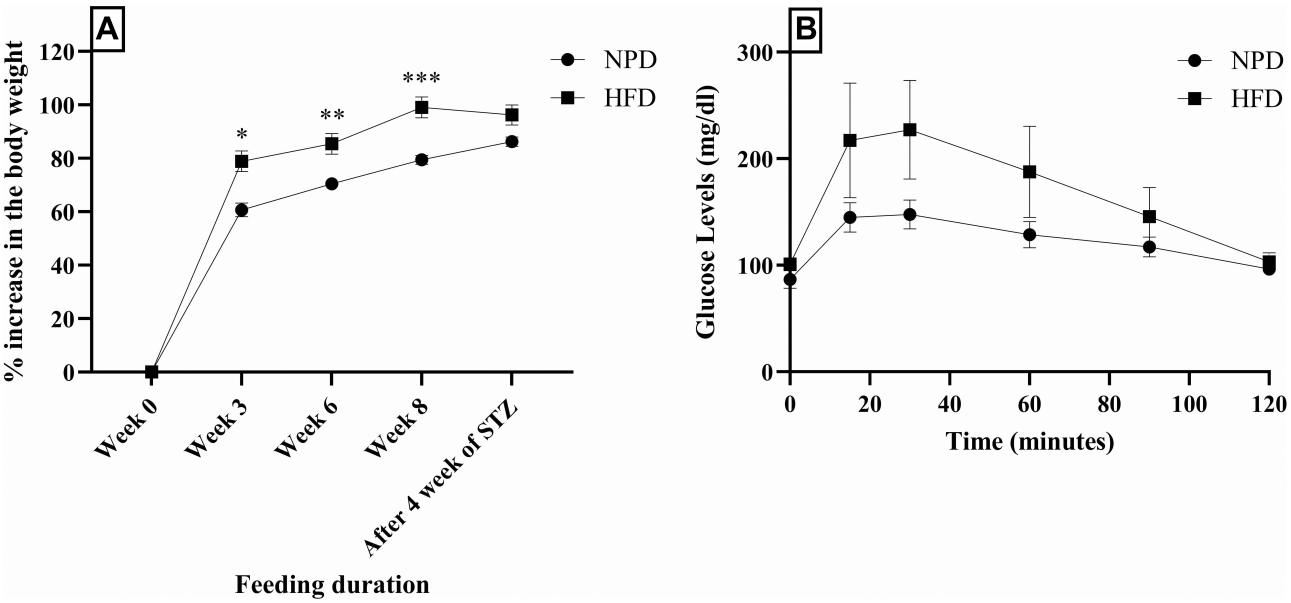

Figure 6 Effect of HFD on (**A**) body weight and (**B**) OGTT. Data represented as mean ± SEM, n=18 (NPD group), n=90 (HFD group). *p<0.05, **p<0.01, ***p<0.0001 when compared to the NPD group. Samples were analysed by two-way ANOVA with Bonferroni post-hoc test.

sesamol and PLGA polymer (Figure 1B) exhibited an endothermic peak at 61.18 °C.

Fourier-Transform Infrared (FTIR)

The obtained IR spectrum of drug showed characteristic absorption peaks at 764.87 cm^{-1} for Di-substitution of phenyl, 813.42 cm^{-1} for out-of-plane CH bending bands, 1035.93 cm^{-1} and 1121 cm^{-1} for symmetric stretching of =C–O–C, C–O–C, respectively. The absorption peaks at 1473.11, 1498.87, and 1639.08 represents CH_2 bending, out-of-plane CH bending of phenyl group, phenyl skeletal frequency, and characteristic peak at 3003.31 represents the unsaturated–CH. These characteristic peaks confirmed the authentication and purity of the drug. The presence of these same peaks in physical mixtures indicates that there is no interaction between drug and polymer. The FTIR spectrum of the pure drug and the physical mixture of drug and excipients is given in Figure 2A and B.

Physicochemical Characterization of Sesamol-PLGA Nanosuspension

Sesamol-PLGA nanosuspension was prepared by emulsification-solvent evaporation technique using stabilizing

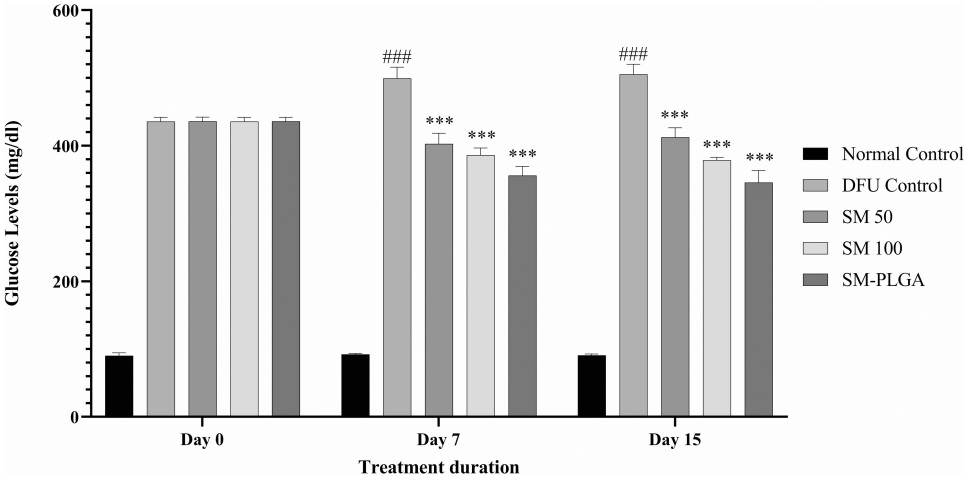

Figure 7 Effect of SM-PLGA nanosuspension on fasting blood glucose in HFD + STZ-induced Type-II diabetic rats. Data represented as mean ± SEM, n=6. ###p<0.001 when compared with NC. ***p<0.001 when compared with the DFU. Samples were analysed by two-way ANOVA with Bonferroni post-hoc test.

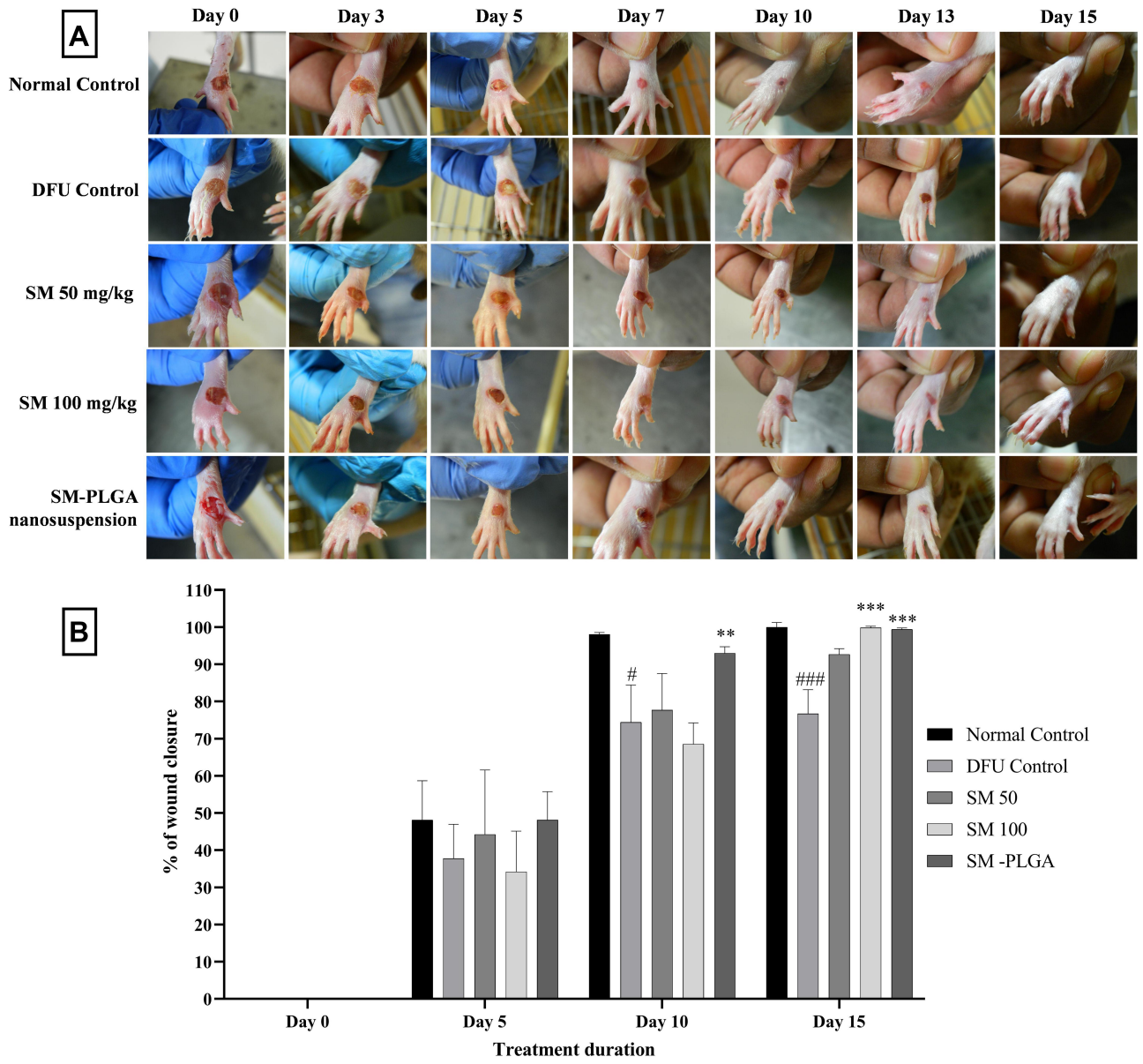

Figure 8 (**A**) Representative images of DFU of treatments at 0, 3, 5, 7, 10, 13 and 15 days (**B**) Effect of SM-PLGA nanosuspension on wound closure in HFD+ STZ induced Type-II diabetic rats. Data represented as mean ± SEM, n=6. $^{\#}p<0.05$, $^{\#\#\#}p<0.001$ when compared with NC, $^{**}p<0.01$ and $^{***}p<0.001$ when compared with the DFU. Samples were analysed by two-way ANOVA with Bonferroni post-hoc test.

agent polyvinyl alcohol. The physicochemical properties of the prepared nanosuspensions are presented in Table 1. The formulation was optimized by using different amount of PLGA, different % of PVA, different amplitude of sonication and different sonication time were used as variable and particle size, PDI, Zeta potential and entrapment efficiencies were evaluated. In the physiochemical characterization, we observed that 200 mg of polymer, 100 mg of sesamol, 1% PVA with 80% amplitude and 5 minutes sonication of formulation with 15000 RPM homogenization yielded desired properties of formulation like the particle size 247 ± 3.64 nm, PDI 0.196 ± 0.052, zeta potential -11.67 ± 0.67 mV and entrapment efficiency was found to be 79.17 ± 0.87% was observed.

Transmission Electron Microscopy

TEM analysis was used in studying the morphology of optimized formulation. The TEM analysis confirmed that the size of the nanoparticles measured in nanometres and all particles found to be spherical in shape and having smooth surface and uniform distribution.

The 50 nm magnification of a single particle showed cage-like structure where drug molecules are dispersed uniformly in polymer matrix and 200 nm magnification showed the particle size is 160 nm, this is may be because of sample preparation for TEM. TEM images recorded at 9900× and 38000× are given in Figure 3A and B, respectively.

In vitro Drug Release Study

Cumulative drug release from the encapsulated drug in the PLGA nanoparticles study is important because restricted release of the drug from polymer matrix may reduce the availability of the drug and efficacy. The in vitro drug release profile of sesamol from PLGA nanosuspension is shown in Figure 4. The cumulative drug release pattern showed biphasic response. Within 24 h, there was a burst release of 62.14% ± 3.62 of the sesamol from PLGA nanoparticles followed by a gradual release of sesamol observed up to 60 h up to 80.19%± 0.64. Sesamol solution showed maximum release within 10 h because of its high aqueous solubility.

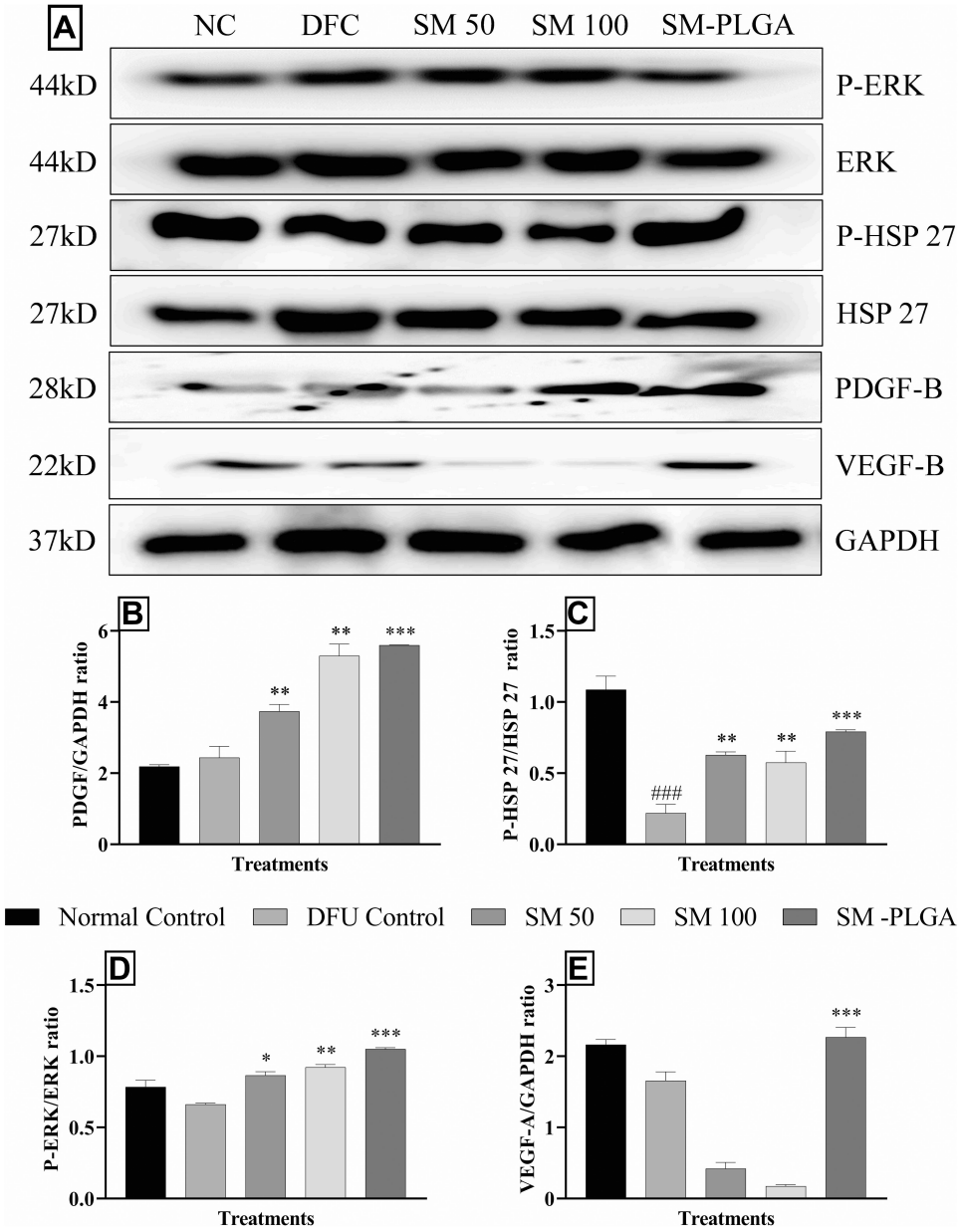

Figure 9 Effect of SM-PLGA nanosuspension on HSP27, ERK, PDGF-B and VEGF expression. (**A**) Representative images of blots; (**B**) PDGFB/GAPDH ratio; (**C**) P-HSP27/HSP27 ratio; (**D**) P-ERK/ERK ratio; (**E**) VEGF/GAPDH ratio. Data represented as mean ± SEM, n=3. ###p<0.001 when compared with NC. *p<0.05, **p<0.01 and ***p<0.001 when compared with the DFU. Samples were analysed by one-way ANOVA with Tukey's post-hoc test.

In vivo Studies

Pharmacokinetic Study

Pharmacokinetic profile of standard drug and formulation is presented in Figure 4 and pharmacokinetic parameters of both the groups are presented in Table 2. C_{max} of the PLGA nanoparticles is decreased in comparison with the standard drug, whereas the time to reach maximum concentration (T_{max}) increased significantly. Area under the curve values were found to be almost the same in both standard and PLGA nanoparticles, but the mean residence time of PLGA nanoparticles increased drastically in comparison with the standard drug. Elimination half-life of PLGA nanoparticles increased significantly in comparison to the standard drug which might be the reason for the slow elimination of the drug from the body. From the plasma concentration and time graph it was evident that standard drug is eliminating from the body within 24 h of dosing, whereas the developed formulation is showing drug in plasma even after 96 h and the elimination rate constant values of both the groups are supporting the statement (Figure 5A and B). Even though the drug is eliminating slowly from the body in formulation group animals, there is not much difference in the AUC values of both standard and formulation groups. This indicates the sustained release of the drug from the nanoparticles.

Development of Type-II Diabetes

Feeding of HFD to the animals caused a gain in the body weight from week 3 onwards comparing to the normal pellet diet (NPD) group, the % increase in body weight continued up to the beginning of the diabetes induction (8th week of HFD feeding). After STZ injection, rats showed weight reduction and control group (NPD group) animals showed increase in body weight (Figure 6A). HFD feeding led to development of insulin resistance as well as impaired clearance of increased blood glucose levels over 2 h blood glucose observation, which was confirmed by OGTT (Figure 6B). OGTT demonstrated minor increase in blood glucose levels during 2 h blood glucose monitoring also showed impaired clearance. The blood glucose levels were significantly high at 15, 30, and 90 min compared to the NPD group. Body weight increase and delay in clearance of acute glucose levels, increase in the blood demonstrates the development of insulin resistance,[22] then after 8 weeks of HFD intervention, animals were injected with STZ injection 35 mg/kg and blood glucose levels measured for four weeks after STZ injection. Animals showing blood glucose levels more than 400 mg/dL were taken into the study and randomized into diabetic foot control (DFU), sesamol 50 mg/kg (SM-50), sesamol 100 mg/kg (SM-100), SM-PLGA suspension (50 mg/kg) and normal control (NC) groups. NC, DC treated with 0.25% CMC, SM-50 group treated with 50 mg/kg, SM-100 group treated with 100 mg/kg and SM-PLGA group treated with 50 mg/kg dose for a period of 15 days after which the blood glucose levels were measured.

Effect of SM-PLGA Nanosuspension on Fasting Blood Glucose Levels

Uncontrolled high blood glucose levels led to microvascular and macrovascular complications[23] like impaired angiogenesis and diabetic neuropathy. In our study, treatment with sesamol and sesamol-PLGA nanosuspension showed a significant decrease in the blood glucose levels compared to the DFU control (Figure 7) and SM-PLGA nanosuspension showed better activity than SM-100 mg/kg due to improved volume of distribution and half-life of sesamol in the formulation.

Effect of SM-PLGA Nanosuspension on Wound Closure

The effects of SM, SM-PLGA on wound healing evaluated in full thickness foot ulcer animal model. The animals were treated with respective treatments for a period of 15 days and wound area was traced on 5th, 10th and 15th day post wounding animals were sacrificed for histological analysis. On 5th day onwards, SM-PLGA nanosuspension showed acceleration in wound healing compared to the DFU, SM-50 and SM-100 though it was not statistically significant. On Day 10 post wounding, SM-PLGA nanosuspension showed almost 92% closure and by Day 15 it was close to 100% (Figure 8A and B). It was statistically significant when compared to the DFU control. At Day 10 and Day 15, DFU group showed only

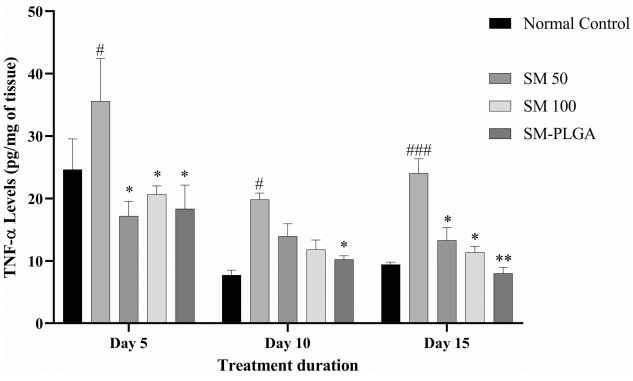

Figure 10 Effect of SM-PLGA nanosuspension on expression of TNF-α levels. Data represented as mean ± SEM, n=3. $^{\#}p<0.5$, $^{\#\#\#}p< 0.001$ when compared with NC. $^{*}p<0.05$, $^{**}p<0.01$ when compared with the DFU. Samples were analysed by one-way ANOVA with Tukey's post-hoc test.

75% wound closure compared to the NC. SM-50 and SM-100 showed 80% and 90% wound closure at Day 15. Thus, SM-PLGA nanosuspension significantly accelerated the wound healing rate compared to the SM-50 and SM-100 groups.

Effect of SM-PLGA Nanosuspension on HSP-27, ERK, PDGF-B and VEGF Expression by Western Blot

Heat Shock Proteins (HSP) are stress activated proteins expressed in cells when exposed to stress. HSP-27 promotes the healing process in wound healing through MAPK signalling by recruiting the dermal fibroblasts at the wound site and restores the homeostasis, however, in diabetic wounds there is down regulation of HSP that takes place which alters the wound healing process.[24] In chronic diabetic conditions, there is evidence that uncontrolled glucose levels cause reduction in the availability of growth factors like PDGF and VEGF at the wound site.[25]

In this study, we demonstrated that in DFU group, phosphorylation of HSP-27 and expression of PDGF and VEGF significantly decreased compared to the NC group whereas sesamol-PLGA nanosuspension significantly increased the phosphorylation levels of HSP-27, ERK and also increased

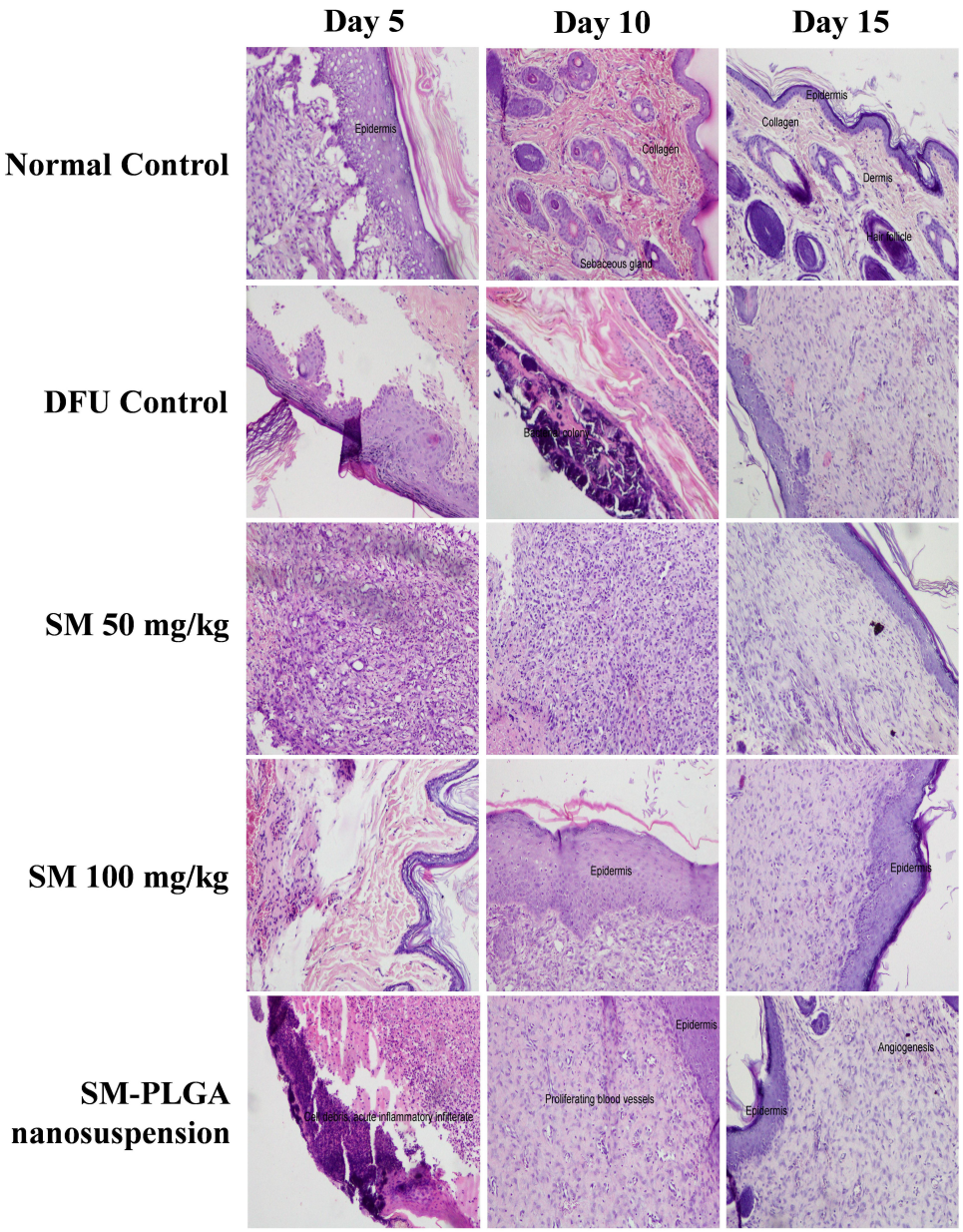

Figure 11 Effect of SM-PLGA nanosuspension on histology (H&E Staining). Images were captured at 400× optical zoom.

the expression of VEGF and PDGF significantly when compared to the DFU and better than SM-50 and SM-100 groups (Figure 9). This protein expression demonstrates that the acceleration of healing process of SM-PLGA in DFU is due to increase in the expression of HSP-27, ERK, PDGF and VEGF.

Effect of SM-PLGA Nanosuspension on TNF-α Expression

In the normal wound healing process, increased levels TNF-α are seen up to 12 to 24 h post wound and elevated levels will normalize after proliferating phase. However, in diabetic conditions, elevation of TNF-α levels is persistent and alters the healing process in diabetic wounds by decreasing the fibroblast proliferation and increasing apoptosis.[26] In the present study, we observed that the TNF-α levels on day 5, day 10 and day 15 post wounding were elevated in the DFU group compared to the NC group. In addition, the TNF-α levels were elevated up to day 15 of post wounding in DFU which is the major cause of slowdown in wound closure (Figure 8B). In SM-50, SM-100 and SM-PLGA nanosuspension groups, elevated TNF-α reduced significantly at day 5, day 10 and day 15, which may be attributed to antioxidant property of sesamol. The SM-PLGA nanosuspension groups showed significant reduction in elevated TNF-α levels compared to the DFU control and it showed better reduction of TNF-α levels compared to SM-50 and SM-100 (Figure 10).

Effect of SM-PLGA Nanosuspension on Histopathological Changes on Wound Healing Process in DFU

Granulation tissue formation, re-epithelization, collagen deposition, fibroblast cell proliferation and angiogenesis are hallmarks for healing of wounds. In this study, histology was done at day 5, day 10 and day 15 samples to see the acceleration of wound healing with the treatments. Thickening of the wound edges and matured collagen formation was observed in treatment groups which was absent in DFU. Matured granulation tissue, collagen deposition and new blood vessel formation was observed in SM-PLGA group at day 10 itself, which is more than plain drug treatment. Infiltration of inflammatory cells were observed up to day 15 in DFU control while less inflammatory cell infiltration was observed in treatment groups at day 10 and day 15 which correlates with the TNF-α levels on the respective days. In SM-PLGA group, increased proliferation of fibroblast cells at wound site were observed (Figure 11). Scoring of histological parameters was done from minimal to moderate to indicate the degree of healing in DFU conditions.[21] DFU treated with SM-50, SM-100 and SM-PLGA nanosuspension were shown better histological scores than DFU control animals (Table 3). Masson's trichome staining was performed to evaluate the collagen deposition in the study. It was observed at day 5 that NC group showed collagen

Table 3 Effect of SM-PLGA on histopathological parameters

	S. No.	Histopathology Parameter	Day 5	Day 10	Day 15
NC	1	Epidermal Regeneration	++	+++	+++
	2	Granulation tissue	+++	+++	+++
	3	Inflammatory cell infiltration	++	+	+
	4	Angiogenesis	+++	++	+++
	5	Proliferation of fibroblast cells	+++	+++	+++
	6	Collagen deposit	++	++	+++
DFU	1	Epidermal Regeneration	+	++	++
	2	Granulation tissue	+	++	++
	3	Inflammatory cell infiltration	++	++	+
	4	Angiogenesis	+	+	+
	5	Proliferation of fibroblast cells	++	++	++
	6	Collagen deposit	+	+	+
SM50	1	Epidermal Regeneration	+	+	+++
	2	Granulation tissue	+++	++	+++
	3	Inflammatory cell infiltration	+++	+++	+
	4	Angiogenesis	++	++	++
	5	Proliferation of fibroblast cells	++	++	++
	6	Collagen deposit	+	+	++
SM100	1	Epidermal Regeneration	++	++	+++
	2	Granulation tissue	+	+++	+++
	3	Inflammatory cell infiltration	+	+	+
	4	Angiogenesis	+	++	++
	5	Proliferation of fibroblast cells	++	++	++
	6	Collagen deposit	+++	++	++
SM-PLGA	1	Epidermal Regeneration	++	+++	+++
	2	Granulation tissue	++	+++	+++
	3	Inflammatory cell infiltration	+++	+	+
	4	Angiogenesis	++	+++	+++
	5	Proliferation of fibroblast cells	++	++	++
	6	Collagen deposit	++	+++	+++

Note: Scoring of histology, + Mild, ++ Moderate, +++ Extensive.

deposition while other groups showed no collagen formation. However, at day 10, collagen deposition was observed in all groups. SM-PLGA group showed more collagen deposition at wound site compared to all the other groups. At day 15, SM-50 and SM-100 showed more collagen formation than other groups (Figure 12).

Effect of SM-PLGA Nanosuspension on Angiogenesis

Angiogenesis is an essential part of the wound healing[27] process and there are several studies suggesting that impaired angiogenesis leads to chronic non-healing wounds in diabetic conditions.[28] CD-31 is cluster differentiation-31, also known as platelet endothelial cell adhesion molecule (PECAM-1), which is an angiogenesis marker expressed on the surface of the endothelial cells. In this study, we performed CD-31 IHC to evaluate the effect of treatments on angiogenesis. We observed that at day 10, DFU group showed fewer number of blood vessels positive for CD-31 (8±2) whereas SM-PLGA group showed high number of cells positive for CD-31 (37±7), SM-50 group showed fewer number of positive for CD-31 (16±4) and SM-100 group showed moderate

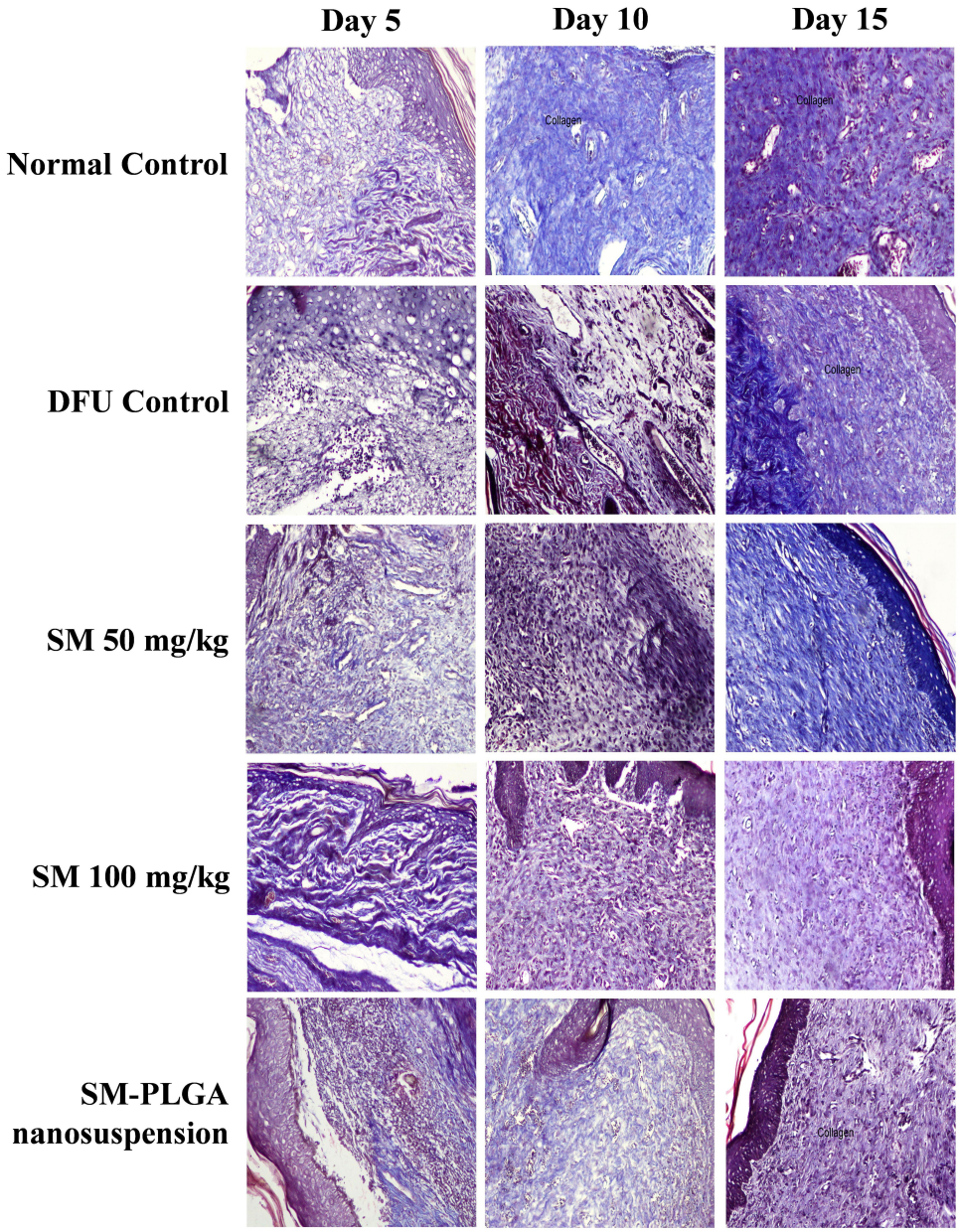

Figure 12 Effect of SM-PLGA nanosuspension on collagen deposition. Images were captured at 400× optical zoom.

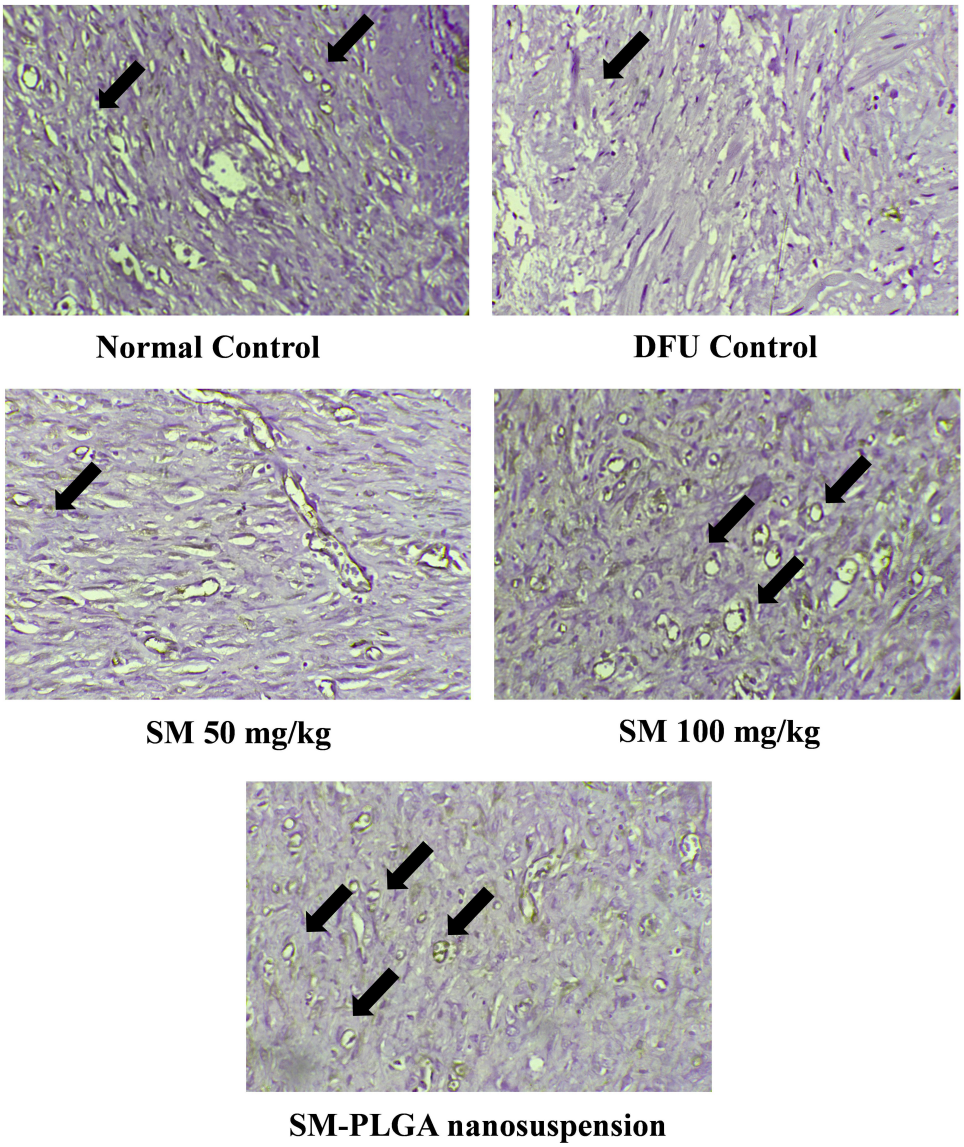

Figure 13 Effect of SM-PLGA nanosuspension on CD-31 expression. Images were captured at 400× optical zoom. Arrows indicate positive cells for CD-31.

number of cells which are positive (28±5) (Figure 13). In Western blot data, SM-50 and 100 groups did not show any effect on VEGF expression. Histology analysis and immunohistochemical analysis suggested that SM-PLGA group showed significant acceleration in wound healing by increasing the reepithelization, granulation tissue formation, fibroblast proliferation and angiogenesis.

Conclusion

The present study investigated the effect of sesamol-PLGA nanosuspension on diabetic foot ulcer animal model. We demonstrated that SM-PLGA nanosuspension is capable of controlled release of sesamol which significantly accelerated the healing process in foot ulcers by down-regulating inflammatory mediators' expression, accelerating the re-epithelization, improved granulation tissue formation, collagen deposition at wound site and increasing the neovascularization. These are all important hallmarks of the wound healing process that led to the rapid closure of wounds within a period of 10 days. This result suggests that SM-PLGA nanoformulation is a promising healing agent for use in the treatment of non-healing chronic wounds.

Acknowledgment

The authors would like to acknowledge the financial support from the Department of Biotechnology (DBT) [BT/Bio-

CARe/01/9610/2013-14]. The authors would also like to acknowledge Department of Pharmacology and Department of Pharmaceutics, Manipal College of Pharmaceutical Sciences, Manipal Academy of Higher Education for providing the infrastructure. We would like to extend our sincere thanks to Evonik India Pvt. Ltd., Mumbai, India for providing the gift sample of PLGA used in this study.

Disclosure

The authors report no conflicts of interest for this work.

References

1. Yang P, Pei Q, Yu T, et al. Compromised wound healing in ischemic type 2 diabetic rats. *PLoS One*. 2016;11(3):e0152068–e0152068. doi:10.1371/journal.pone.0152068
2. Guo S, Dipietro LA. Factors affecting wound healing. *J Dent Res*. 2010;89(3):219–229. doi:10.1177/0022034509359125
3. Majdalawieh AF, Mansour ZR. Sesamol, a major lignan in sesame seeds (Sesamum indicum): anti-cancer properties and mechanisms of action. *Eur J Pharmacol*. 2019;855:75–89. doi:10.1016/j.ejphar.2019.05.008
4. Kumar N, Mudgal J, Parihar VK, Nayak PG, Kutty NG, Rao CM. Sesamol treatment reduces plasma cholesterol and triacylglycerol levels in mouse models of acute and chronic hyperlipidemia. *Lipids*. 2013;48(6):633–638.
5. Parihar VK, Prabhakar KR, Veerapur VP, et al. Effect of sesamol on radiation-induced cytotoxicity in Swiss albino mice. *Mutat Res Genet Toxicol Environ Mutagen*. 2006;611(1):9–16. doi:10.1016/j.mrgentox.2006.06.037
6. Shenoy RR, Sudheendra AT, Nayak PG, Paul P, Kutty NG, Rao CM. Normal and delayed wound healing is improved by sesamol, an active constituent of Sesamum indicum (L.) in albino rats. *J Ethnopharmacol*. 2011;133(2):608–612. doi:10.1016/j.jep.2010.10.045
7. Jan K-C, Ho C-T, Hwang LS. Bioavailability and tissue distribution of sesamol in rat. *J Agric Food Chem*. 2008;56(16):7032–7037. doi:10.1021/jf8012647
8. Jan K-C, Ho C-T, Hwang LS. Elimination and metabolism of sesamol, a bioactive compound in sesame oil, in rats. *Mol Nutr Food Res*. 2009;53(S1):S36–S43. doi:10.1002/mnfr.200800214
9. Geetha T, Singh N, Deol PK, Kaur IP. Biopharmaceutical profiling of sesamol: physiochemical characterization, gastrointestinal permeability and pharmacokinetic evaluation. *RSC Adv*. 2015;5(6):4083–4091. doi:10.1039/C4RA10926K
10. Shao M, Hussain Z, Thu HE, et al. Emerging Trends in Therapeutic Algorithm of Chronic Wound Healers: Recent Advances in Drug Delivery Systems, Concepts-to-Clinical Application and Future Prospects. *Crit Rev Ther Drug Carrier Syst*. 2017;34(5):387–452. doi:10.1615/CritRevTherDrugCarrierSyst.2017016957
11. Hussain Z, Thu HE, Shuid AN, Katas H, Hussain F. Recent advances in polymer-based wound dressings for the treatment of diabetic foot ulcer: an overview of state-of-the-art. *Curr Drug Targets*. 2018;19(5):527–550. doi:10.2174/1389450118666170704132523
12. Hussain Z, Thu HE, Ng SF, Khan S, Katas H. Nanoencapsulation, an efficient and promising approach to maximize wound healing efficacy of curcumin: a review of new trends and state-of-the-art. *Colloids Surf B Biointerfaces*. 2017;150:223–241. doi:10.1016/j.colsurfb.2016.11.036
13. Kola Srinivas NS, Verma R, Pai Kulyadi G, Kumar L. A quality by design approach on polymeric nanocarrier delivery of gefitinib: formulation, in vitro, and in vivo characterization. *Int J Nanomedicine*. 2016;12:15–28. doi:10.2147/IJN.S122729
14. Hirpara MR, Manikkath J, Sivakumar K, et al. Long circulating PEGylated-chitosan nanoparticles of rosuvastatin calcium: development and in vitro and in vivo evaluations. *Int J Biol Macromol*. 2018;107:2190–2200. doi:10.1016/j.ijbiomac.2017.10.086
15. Fernandes AV, Pydi CR, Verma R, Jose J, Kumar L. Design, preparation and in vitro characterizations of fluconazole loaded nanostructured lipid carriers. *Braz J Pharm Sci*. 2020;56.
16. Bairagi U, Mittal P, Singh J, Mishra B. Preparation, characterization, and in vivo evaluation of nano formulations of ferulic acid in diabetic wound healing. *Drug Dev Ind Pharm*. 2018;44(11):1783–1796. doi:10.1080/03639045.2018.1496448
17. Srinivasan K, Viswanad B, Asrat L, Kaul CL, Ramarao P. Combination of high-fat diet-fed and low-dose streptozotocin-treated rat: a model for type 2 diabetes and pharmacological screening. *Pharmacoll Res*. 2005;52(4):313–320. doi:10.1016/j.phrs.2005.05.004
18. Shi R, Lian W, Han S, et al. Nanosphere-mediated co-delivery of VEGF-A and PDGF-B genes for accelerating diabetic foot ulcers healing in rats. *Gene Ther*. 2018;25(6):425–438. doi:10.1038/s41434-018-0027-6
19. Hemalatha G, Pugalendi KV, Saravanan R. Modulatory effect of sesamol on DOCA-salt-induced oxidative stress in uninephrectomized hypertensive rats. *Mol Cell Biochem*. 2013;379(1):255–265. doi:10.1007/s11010-013-1647-1
20. Vennila L, Pugalendi KV. Protective effect of sesamol against myocardial infarction caused by isoproterenol in Wistar rats. *Redox Rep*. 2010;15(1):36–42. doi:10.1179/174329210X12650506623168
21. Muhammad AA, Arulselvan P, Cheah PS, Abas F, Fakurazi S. Evaluation of wound healing properties of bioactive aqueous fraction from Moringa oleifera Lam on experimentally induced diabetic animal model. *Drug Des Devel Ther*. 2016;10:1715–1730. doi:10.2147/DDDT.S96968
22. Reed MJ, Meszaros K, Entes LJ, et al. A new rat model of type 2 diabetes: the fat-fed, streptozotocin-treated rat. *Metabolism*. 2000;49(11):1390–1394. doi:10.1053/meta.2000.17721
23. Fowler MJ. Microvascular and macrovascular complications of diabetes mellitus. *Clin Diabetes*. 2006;26(2):77–82. doi:10.2337/diaclin.26.2.77
24. Singh K, Agrawal NK, Gupta SK, et al. Decreased expression of heat shock proteins may lead to compromised wound healing in type 2 diabetes mellitus patients. *J Diabetes Complications*. 2015;29(4):578–588. doi:10.1016/j.jdiacomp.2015.01.007
25. Brem H, Tomic-Canic M. Cellular and molecular basis of wound healing in diabetes. *J Clin Invest*. 2007;117(5):1219–1222. doi:10.1172/JCI32169
26. Xu F, Zhang C, Graves DT. Abnormal cell responses and role of TNF-α in impaired diabetic wound healing. *Biomed Res Int*. 2013;2013:754802. doi:10.1155/2013/754802
27. Tonnesen MG, Feng X, Clark RAF. Angiogenesis in wound healing. *J Investig Dermatol Symp Proc*. 2000;5(1):40–46. doi:10.1046/j.1087-0024.2000.00014.x
28. Pastar I, Ojeh N, Glinos GD, Stojadinovic O, Tomic-Canic M. Physiology and pathophysiology of wound healing in diabetes. In: Veves A, Giurini JM, Guzman RJ, editors. *The Diabetic Foot: Medical and Surgical Management*. Cham: Springer International Publishing; 2018:109–130.